Journal of Molecular Catalysis A: Chemical 379 (2013) 315–321

Contents lists available at ScienceDirect

Journal of Molecular Catalysis A: Chemical

journal homepage: www.elsevier.com/locate/molcata

Selective oxidation of Mandelic acids catalyzed by copper (II) complexes

Wei-Feng Yu, Xiang-Guang Meng*, Xiao Peng, Xiao-Hong Li, Ying Liu

Key Laboratory of Green Chemistry and Technology, Ministry of Education, College of Chemistry, Sichuan University, Chengdu 610064, PR China

ARTICLE INFO

Article history:
Received 20 March 2013
Received in revised form 24 August 2013
Accepted 4 September 2013
Available online 12 September 2013

Keywords:
Hydroperoxo free radical
Lignin
Mandelic acids
Selective oxidation
DFT

ABSTRACT

Two copper (II) complexes L^1Cu and L^2Cu (H_2L^1 = 4,9-dimethyl-2,11-dioxy-5,8-diazacycldode-2,4,8,10-tetraene; H_2L^2 = diethyl-3,8-dimethyl-4,7-diazadeca-2,8-diene-1,10-dioat) were prepared and displayed good catalytic efficiency for the oxidations of Mandelic acid (MA), 4-hydroxymandelic acid (4-HMA) and 4-methoxymandelic acid (4-MMA) by H_2O_2 in aqueous solution at 35 °C. The apparent first-order rate constants k_{obs} of oxidations of MA, 4-HMA and 4-MMA were obtained in the range of pH 2.5–4.5. It was great interesting that the complexes LCu displayed excellent catalytic ability for the selective oxidation of Mandelic acids into aromatic aldehydes (S > 98%). The active species generated by reacting copper (II) complexes LCu with H_2O_2 was characterized by UV–vis, electrospray ionization mass spectrometry (ESI-MS) and cyclic voltammetry (CV). The LCu^{I}-•OOH species was suggested as the possible active species. The geometric configurations of LCu and the LCu^{I}-•OOH species were calculated with Density Functional Theory (DFT) method. The LCu^{I}-•OOH species is stable and possesses relatively high oxidation potential in aqueous solution at ambient temperature. This study also provides a new insight for the degradation of lignin.

1. Introduction

Metal-oxo species are very important active intermediates in biological and biomimetic oxidation reactions [1–4]. In many biological metabolic processes, the generation and long-time stability of the copper-hydroperoxo species are extremely important for those enzyme catalytic oxidation reactions [5–8]. However, the knowledge about the generation, properties and catalysis mechanism of the copper-hydroperoxo species is still not enough. In last decade, some copper-oxo species derived from the oxidation states of copper complex oxidized by O_2 or H_2O_2, such as Cu^{II}-O_2^{-}, Cu^{II}-O• and Cu^{II}-OOH species, were widely studied [9–12]. Recently Comba et al. found a new mononuclear bispidine copper-hydroperoxo species and investigated its some spectroscopic properties [13]. Choi et al. reported the synthesis and properties of copper-hydroperoxo species bearing a Me_6-tren ligand and found it was inactive for electrophilic and nucleophilic oxidation reactions [14]. Fujii et al. found that the reactivity of copper-hydroperoxo species with N_3O-type ligand was greatly influenced by their geometries, the reactivity of the species with square planar geometry was apparently larger than that of the species with the trigonal bipyramidal configuration [15]. In previous reports, metal-hydroperoxo species were generally studied in organic solvent at low temperature, owing to the instability and complexity in aqueous solution at ambient temperature [16–19]. Schepetkin et al. reported that several free radical species •OOH, $O_2^{\bullet-}$ and •OH could be formed in the aqueous solution containing copper (II) complex and hydrogen peroxide [20]. Lin and Wu suggested that the hydroperoxo free radical associates with the center copper ion to form copper-peroxo or copper-hydroperoxo species [21]. Some researchers also found that the formation of copper-hydroperoxo species could be influenced by many factors including catalysts, pH of the solution, solvent and temperature [22–24]. However until now, under what condition the copper-hydroperoxo species can be generated primarily is still unclear. In previous studies [25], we found that the "copper complex associative radical" LCu^{I}-•OOH may be the predominant oxidation species which is the oxidation state of copper complex oxidized by H_2O_2 in buffer solution. In present work, this kind of LCu^{I}-•OOH species could be easily generated by the reaction of copper complex with H_2O_2 in tartaric acid buffer solution at ambient temperature. Some properties of this species were also investigated in detail.

Mandelic acids are widely used as typical model substrate of lignin degradation enzymes [26–28]. The efficient degradation of lignin and its separation from the lignocellulose are challenging problems encountered in biofuel production, lignin contains lots of units of –OH and/or $–OCH_3$ substituted aromatic secondary alcohols [29,30]. Recently we adopted a new route to degrade lignin by

* Corresponding author. Tel.: +86 28 85462979; fax: +86 28 85412907.
E-mail address: mengxgchem@163.com (X.-G. Meng).

1381-1169/$ – see front matter © 2013 Elsevier B.V. All rights reserved.
http://dx.doi.org/10.1016/j.molcata.2013.09.004

selective oxidations of aromatic secondary alcohols and aromatic ketones under mild condition [31,32]. In present work, we found that the "copper complex associative radical" LCu^{I}-•OOH species could be readily generated and exhibited an excellent selectivity for the oxidation of Mandelic acids by H_2O_2.

2. Experimental

2.1. Materials

Mandelic acid (MA), 4-hydroxymandelic acid (4-HMA), 4-methoxymandelic acid (4-MMA), 30% hydrogen peroxide, benzaldehyde, 4-hydroxybenzaldehyde, anisaldehyde, ethyl 3-oxobutanoate, pentane-2,4-dione, ethane-1,2-diamine, sodium hydroxide, tartaric acid were all analytical grade and purchased from the commercial sources. All other chemicals and solvents used were also analytical grade without further purification.

2.2. Synthesis of ligands and preparation of copper (II) complexes

The ligand H_2L^1 (4,9-dimethyl-2,11-dioxy-5,8-diazacy-cldode-2,4,8,10-tetraene) $C_{12}H_{20}N_2O_2$ and H_2L^2 (diethyl-3,8-dimethyl-4,7-diazadeca-2,8-diene-1,10-dioat) $C_{14}H_{24}N_2O_4$ were synthesized according to literatures [33,34].

The copper (II) complex L^1Cu and L^2Cu were prepared according to the reported methods [33,35,36]. The data of ligands and copper complexes are listed in Table 1

2.3. Instrumentations and methods

Ultraviolet–visible absorbance measurements were performed with a Hitachi U-2910 spectrophotometer (Tokyo, Japan). Electrochemical measurements were performed using a CHI660C electrochemical analyzer. All cyclic voltammetry (CV) measurements were carried out with a three-electrode-system with a small glassy carbon as working electrode, a Pt wire counter electrode and a KCl saturated calomel electrode reference electrode all being placed into the solution. ^{1}H NMR spectra were recorded on a Bruker spectrometer, using $CDCl_3$ as an internal standard. Elemental analyses were implemented with a Carlo Erba 1106 instrument. The FT-IR spectrum was measured by Fourier transform infrared spectrometer (FT-IR, NEXUS 6700, USA).

The typical reaction solution containing 0.05 mmol L^{-1} copper (II) complex, 0.03 mol L^{-1} hydrogen peroxide and 0.001 mol L^{-1} Mandelic acids were kept at constant 35 °C in the tartaric acid buffer solution. Test samples were extracted from the reactor periodically. The concentrations of benzaldehyde (ε_{300} = 652 L mol^{-1} cm^{-1}), 4-hydroxybenzaldehyde (ε_{300} = 10 000 L mol^{-1} cm^{-1}) and anisaldehyde (ε_{300} = 9500 L mol^{-1} cm^{-1}) in the reaction solution were determined by UV–vis analysis at wavelength 300 nm. MA, 4-HMA and 4-MMA had no spectral absorbance contribution at 300 nm. The mixture reaction solution, extracted with CH_2Cl_2 and dried over Na_2SO_4, was analyzed by GC (GC9790, Fu li, China), GC–MS (Agilent 5973 Network 6890 N) and HPLC (waters 1525) with a UV–vis detector. GC measure conditions: KB-5 capillary column; carrier gas, N_2; gasification temperature, 300 °C; the column temperature is programmed to keep at 60 °C for 2 min, then rise to 60–300 °C (25 °C/min); injection volume, 0.2 μL. GC–MS measure conditions: DB-5 capillary column; carrier gas, N_2: 60 cm^3 min^{-1}, He: 2.0 cm^3 min^{-1}; gasification temperature, 300 °C; the column temperature is programmed to keep at 40 °C for 4 min, then rise to 40–260 °C (15 °C/min); injection volume, 0.1 μL. HPLC measure conditions: C18 column; mobile phase, methanol/water (V/V = 1/1), 0.5 ml min^{-1}; column temperature, 30 °C; injection volume, 20 μL; UV detection wavelength, 280 nm.

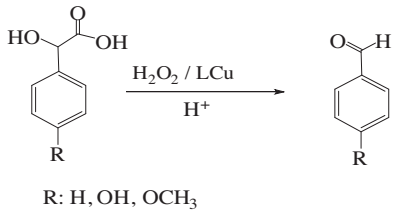

Scheme 1. Selective catalytic oxidation of Mandelic acids to aromatic aldehyde.

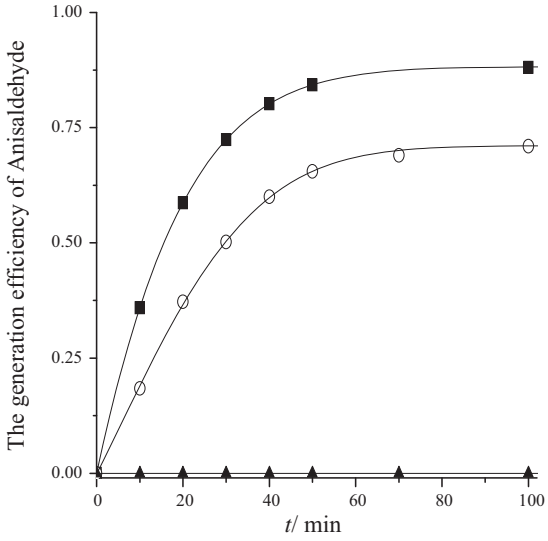

Fig. 1. The generation of anisaldehyde catalyzed by LCu at pH 3 and 35 °C; C_0(4-MMA) = 1 mmol L^{-1}, $C_0(H_2O_2)$ = 0.03 mol L^{-1}, C_0(LCu) = 0.05 mmol L^{-1}. (■) L^1Cu, (○) L^2Cu, (▲) without catalyst.

2.4. Computation

All Density Functional Theory (DFT) calculations were performed with the Gaussian 03 programs. Geometry optimizations were carried out at the >B3LYP/6-311++G(d, p), SDD level.

3. Results and discussion

3.1. Selective oxidation of Mandelic acids catalyzed by complexes LCu

Lignin is one main component in lignocellulose. Up to now, its efficient degradation is still a challenging problem in the utilization of biomass [29,30]. MA, 4-HMA, 4-MMA, which are aromatic secondary alcohols, were widely used as typical model substrates of lignin [26–28]. In present work, we employed the copper complexes L^1Cu and L^2Cu to catalyze the oxidation of Mandelic acids by H_2O_2 (Scheme 1). Fig. 1 showed the formation process of anisaldehyde catalyzed by complexes LCu. From Fig. 1, it could be seen that the oxidation reaction of 4-MMA with H_2O_2 was hardly occurred, however the presence of catalyst LCu rapidly accelerated the reaction. The mixture reaction solution extracted with CH_2Cl_2 and dried by Na_2SO_4. The product of the reaction was analyzed by GC–MS (see Fig. S2) and HPLC (Fig. 2). The analysis results indicated that anisaldehyde was the only detectable product, the selectivity of anisaldehyde was more than 98%. The oxidation reactions of other two Mandelic acids (MA and 4-HMA) with H_2O_2 catalyzed by LCu displayed the same characteristics as that of 4-MMA. The benzaldehyde or 4-hydroxybenzaldehyde is the sole detectable product. The selectivity was more than 98% (the error was evaluated less than 2%).

Table 1
Color, Mp, ^{1}H NMR, IR data, ICP-AES data, elemental analyses of the ligands and copper complexes.

Compound	Color	Mp (°C)	^{1}H NMR, δ	IR data (KBr, mmax/cm^{-1})	ICP-AES % Cu	Elemental analyses % Found (calculated) C H N
H_2L^1	Light yellow crystal	113 °C	1.89 (s, 6H, CH_3), 2.01 (s, 6H, CH_3), 3.42 (d, 4H, CH_2), 4.99 (s, 2H, CH), 10.99 (s, 2H, NH).	738 m, 851 m, 1288 vs, 1516 vs, 1577 vs, 1610 vs, 2948 m, 2996 m, 3083 m, 3159 m, 3450 br.	–	64.30 8.96 12.45 (64.26 8.99 12.49)
H_2L^2	Colorless crystal	132 °C	1.26 (t, 6H, CH_3), 1.93 (s, 6H, CH_3), 3.37 (m, 4H, CH_2), 4.12 (q, 4H, CH_2), 4.50 (s, 2H, CH), 8.66 (s, 2H, NH).	724m, 784 s, 1169 s, 1289 vs, 1605 vs, 1648 vs, 2897 m, 2952 s, 2986 s, 3296 s.	–	59.09 8.48 9.90 (59.13 8.51 9.85)
L_1Cu	Green	145 °C	–	453 w, 780 m, 1021 w, 1275 w, 1405 s, 1530 s, 1578 vs, 3165 br, 3444 br.	22.24	50.53 6.40 9.74 (50.42 6.35 9.80)
L_2Cu	Purple	158 °C	–	488 m, 769 m, 1069 m, 1290 s, 1425 s, 1468 vs, 1508 vs, 1583 vs, 3168 br, 3450 br.	18.45	48.68 6.32 8.06 (48.61 6.41 8.10)

IR data, br: broad, s: strong, vs: very strong, m: medium, w: weak.

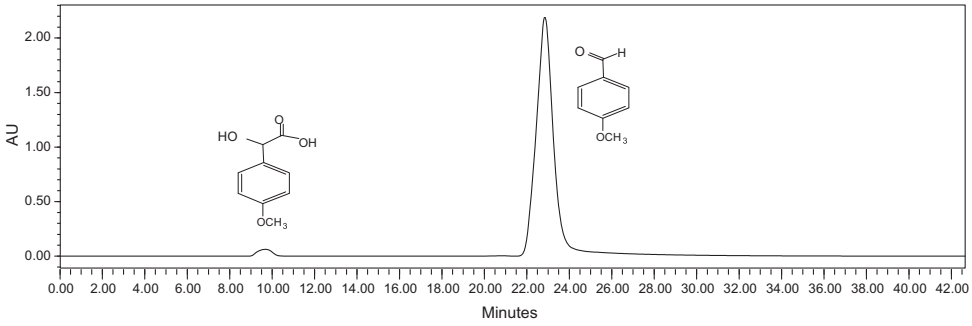

Fig. 2. HPLC profile of the reaction solution after 2 h.

In order to investigate the reaction kinetics, we employed excessive concentration of H_2O_2 over that of 4-MMA to carry out the reaction. The apparent first-order formation rate constants k_{obs} were calculated based on the plots of $\ln[(A_\infty - A_0/A_\infty - A_t)]$ vs reaction time t (Fig. 3), where A_0 and A_t were the absorbance of reaction product anisaldehyde at time 0 and t respectively. A_∞ was the absorbance of anisaldehyde at the same concentration with that of C_0(4-MMA). From Fig. 3 it can be seen that the plots of $\ln[(A_\infty - A_0)/(A_\infty - A_t)]$ vs time t were all straight lines and approximately passed the origin (the correlative coefficients $r > 0.995$), which indicated this was a first-order reaction with respect to the concentrations of 4-MMA for the initial reaction time 15 min. In this work, in order to avoid the influences of the decomposition of H_2O_2 on reaction, the experimental data for the initial 15 min reaction time were employed to calculate the anisaldehyde formation rate constants. The calculated apparent first-order rate constants k_{obs} of formation of benzaldehyde, 4-hydroxybenzaldehyde and anisaldehyde were listed in Table 2.The initial benzaldehyde, 4-hydroxybenzaldehyde and anisaldehyde formation rates k_{obs} were affected by pH values of solution. From Table 2, it can be seen that the initial aromatic aldehyde formation rate constants k_{obs} increased with decreasing pH. The pH effect may attribute to both protonation of substrate Mandelic acids and generation of active species under acidic aqueous solution, as illustrated in Scheme 2. We also investigated the oxidation reaction in neutral and weak alkaline solutions, when pH > 8 several active species including superoxide anion free radical, hydroperoxo free radical, hydroxide radical could be generated simultaneously in the aqueous solution and the reaction products became complex.

3.2. The generation and solution properties of active species

The active copper-oxo species played an important role in catalytic oxidation reaction. In order to obtain the information of the

Table 2
Apparent first-order rate constants k_{obs} of formation of aromatic aldehyde at 35 °C.[a]

pH	L^1Cu			L^2Cu		
	MA	4-HMA	4-MMA	MA	4-HMA	4-MMA
	$10^4 k_{obs}$ (s^{-1})			$10^4 k_{obs}$ (s^{-1})		
2.5	2.91	5.72	11.7	0.85	2.18	3.86
3.0	2.16	4.07	8.35	0.66	1.75	2.89
3.5	1.63	3.27	6.69	0.42	1.08	2.03
4.0	1.45	2.56	5.48	0.29	0.78	1.36
4.5	1.12	2.08	4.57	0.23	0.65	1.02

[a] C_0(MA) = 1 mmol L^{-1}, C_0(4-HMA) = 1 mmol L^{-1}, C_0(4-MMA) = 1 mmol L^{-1}, $C_0(H_2O_2)$ = 0.03 mol L^{-1}, C_0(LCu) = 0.05 mmol L^{-1}.

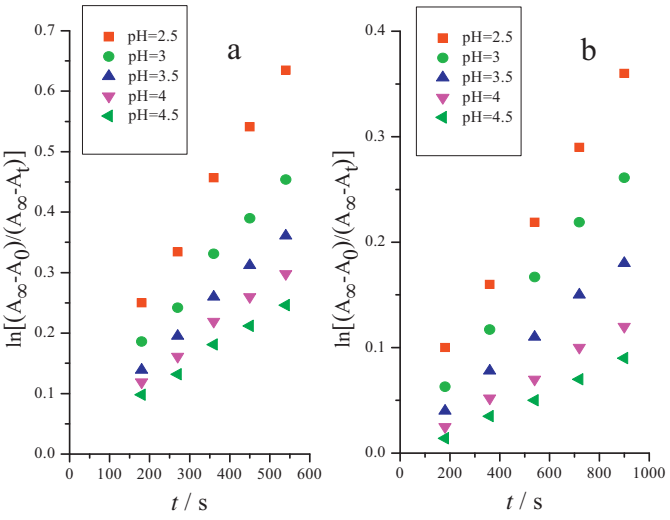

Fig. 3. Plots of $\ln[(A_\infty - A_0)/(A_\infty - A_t)]$ vs reaction time t for the oxidations of 4-MMA by H_2O_2 using L^1Cu (a) and L^2Cu (b) as catalyst in tartaric acid solution at 35 °C. C_0(4-MMA) = 1 mmol L^{-1}, $C_0(H_2O_2)$ = 0.03 mol L^{-1}, C_0(LCu) = 0.05 mmol L^{-1}.

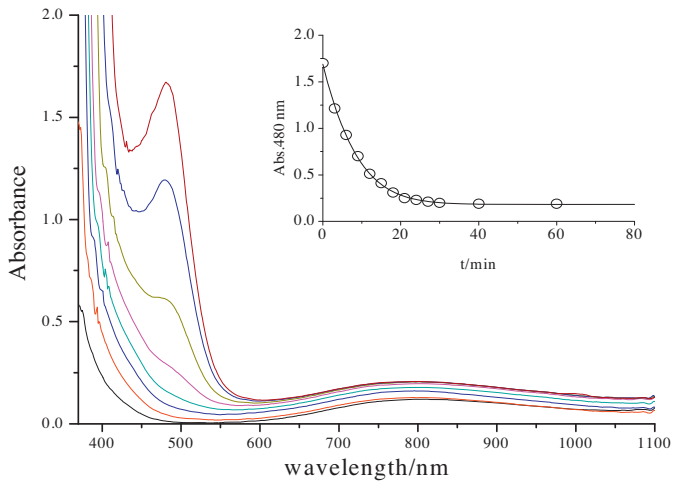

Fig. 5. The UV–vis spectral changes showing the formation of the L^2Cu^I-•OOH species vs time in tartaric acid solution at 25 °C, pH = 3, $C_0(H_2O_2)$ = 0.02 mol L^{-1}, $C_0(L^2Cu)$ = 5 mmol L^{-1}. Inset: time course of the absorbance change of the L^2Cu^I-•OOH species at 480 nm for the reaction with 4-MMA, C_0(4-MMA) = 0.1 mol L^{-1}.

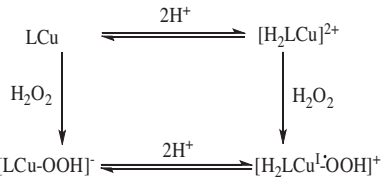

Scheme 2. The possible proton transfer balances and reaction paths.

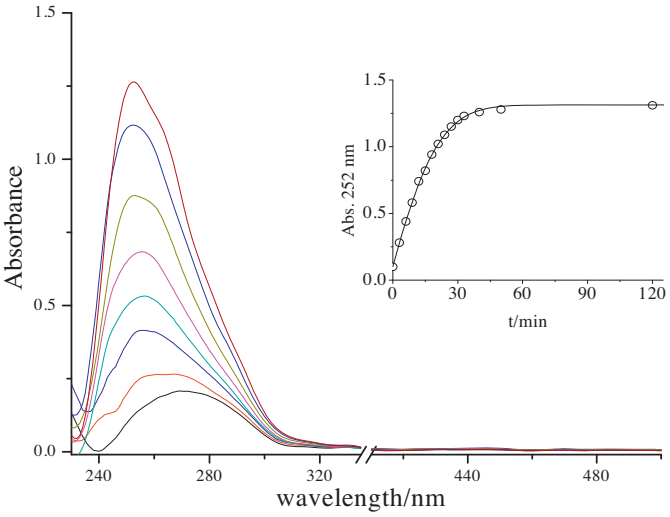

Fig. 4. The UV–vis spectral changes showing the formation of the L^1Cu^I-•OOH species vs time t in tartaric acid solution at 25 °C, pH = 3, $C_0(H_2O_2)$ = 0.2 mmol L^{-1}, $C_0(L^1Cu)$ = 0.05 mmol L^{-1}. Inset: the generation of the L^1Cu^I-•OOH species and the absorbance change at 252 nm vs time t.

LCu^I-•OOH species, the generation and properties of the species were investigated in detail.

The reaction processes of L^1Cu with 4 equiv. H_2O_2 were monitored by UV–vis in tartaric acid solution at 25 °C. The spectral changes were shown in Fig. 4. It can be observed that an optic feature with λ_{max} = 252 nm appeared after adding H_2O_2 to the L^1Cu complex solution. This indicated that a new species formed. Further the formation kinetics showed that the new species could be readily generated within 30 min and then could stably exist for more than 2 h (Fig. 4). It was also found that an optic feature with λ_{max} = 780 nm appeared and simultaneously an optic feature with λ_{max} = 980 nm decreased in the infrared region, isosbestic points were observed at 605 nm and 870 nm (see Fig. S3). These indicated a new stable species formed in aqueous solution at 25 °C. It was noted that the generated species could slowly decompose when it was placed in the aqueous solution beyond 3 h at ambient temperature.

Similarly, after H_2O_2 was added to the L^2Cu complex solution, an UV–vis spectral feature with λ_{max} = 480 nm was observed and simultaneously an optical feature with λ_{max} = 800 nm increased (Fig. 5). From Figs. 4 and 5, we found that although the structure of L^2Cu was similar to that of L^1Cu, the characteristic UV spectrum of species L^2Cu^I-•OOH was different from that of L^1Cu, this implied that ligand L could cause sensitive influence to the copper-oxo species. From Fig. 5, it could be seen that the new species could be rapidly reduced by 4-MMA, the reaction followed a pseudo-first-order kinetic behavior in the case of excessive 4-MMA and the pseudo-first-order rate constant of 2.3×10^{-3} s^{-1} was estimated under the experimental conditions as in Fig. 5.

According to the investigations of UV–vis absorbance, a new active species could be found under this condition. In order to identify the new species further, the reaction aqueous solution was detected by electrospray ionization mass spectrometry (ESI-MS) at ambient temperature. The spectrum of positive ion (see Fig. S4) showed a ion peak at m/z of 319.25 attributed to $[H_2L^1Cu^I$-•OOH$]^+$ (Calc. m/z of 320.08), a peak at m/z of 374.31 attributed to $[H_2L^1Cu^I$-•OOH$(3H_2O)]^+$ (Calc. m/z of 374.11) and a peak at m/z of 390.29 attributed to $[H_2L^1Cu^I$-•OOH$(2H_2O)(H_2O_2)]^+$ (Calc. m/z of 390.11). It could be observed that the reaction of L^1Cu with H_2O_2 results in the formation of $[H_2L^1Cu^I$-•OOH$]^+$ species. The spectrum of negative ion (Fig. S6) showed an anion peak at m/z of 334.93 attributed to $[L^1Cu^I$-OOH$(H_2O)]^-$ (Calc. m/z of 336.07) and a peak at m/z of 486.88 attributed to $[L^1Cu^I$-OOH$(2H_2O_2)(N(C_2H_5)_3)]^-$ (Calc. m/z of 487.20). Similarly, according to the ESI-MS spectrum of positive ion for the reaction solution of L^2Cu with H_2O_2, a prominent peak corresponding to $[H_2L^2Cu^I$-•OOH$]^+$ appeared at m/z of 377.13 (Calc. m/z of 380.10) (see Fig. S5). It could be found that the other two peaks at m/z of 399.15 and m/z of 499.29 attributed to $[H_2L^2Cu^I$-•OOH$(H_2O)]^+$ (Calc. m/z of 398.11) and $[H_2L^2Cu^I$-•OOH$(H_2O)(3H_2O_2)]^+$ (Calc. m/z of 500.13), respectively. This indicated the generation of $[H_2L^2Cu^I$-•OOH$]^+$ derived from the interaction of L^2Cu with H_2O_2. It was very possible that there were different state forms due to the proton transfer between

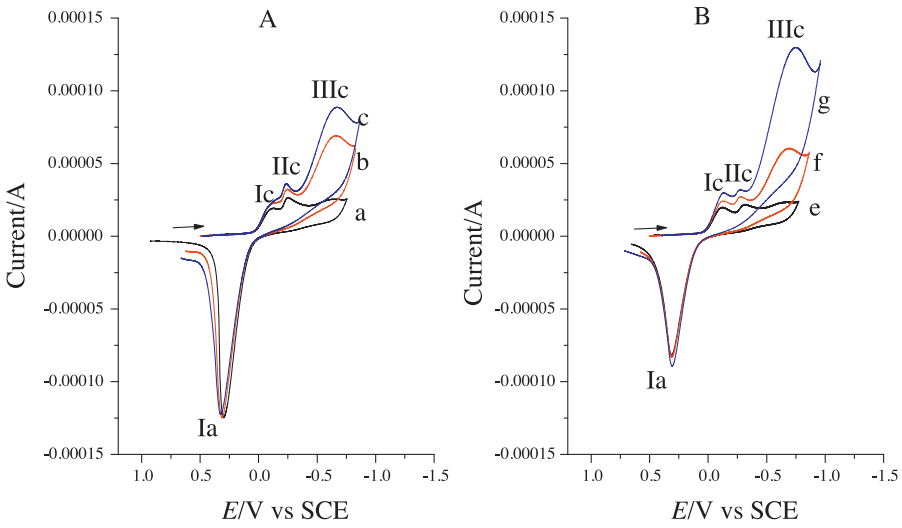

Fig. 6. Cyclic voltammogram of 1 mmol L^{-1} LCu and addition of different amounts of H_2O_2 at a scan rate of 100 mV s^{-1} in unstirred deaerated tartaric acid solution at 25 °C; pH = 3; A: L^1Cu, a: 0 mmol L^{-1} H_2O_2, b: 3 mmol L^{-1} H_2O_2, c: 6 mmol L^{-1} H_2O_2; B: L^2Cu, e: 0 mmol L^{-1} H_2O_2, f: 5 mmol L^{-1} H_2O_2, g: 10 mmol L^{-1} H_2O_2.

LCu and $[H_2LCu]^{2+}$ or between $[LCu\text{-}OOH]^{-}$ and $[H_2LCu^{I}\text{-}^{\bullet}OOH]^{+}$ in aqueous solution as shown in Scheme 2.

Further evidence for the formation of the $LCu^{I}\text{-}^{\bullet}OOH$ species was obtained with electrochemical method. We attempted to identify voltammetric responses corresponding to the active species by titration experiments by adding different amounts of H_2O_2 to the aqueous solutions of LCu. The results were shown in Fig. 6. Incremental addition of H_2O_2 to the solution of L^1Cu resulted in a new increasing reduction wave at E_{pIIIc} = −0.65 V/SCE (Fig. 6A). Similarly, Fig. 6B showed the current responses of L^2Cu in the absence and presence of H_2O_2. From Fig. 6B, a new increasing reduction wave at E_{pIIIc} = −0.67 V/SCE with the addition of H_2O_2 can be observed,

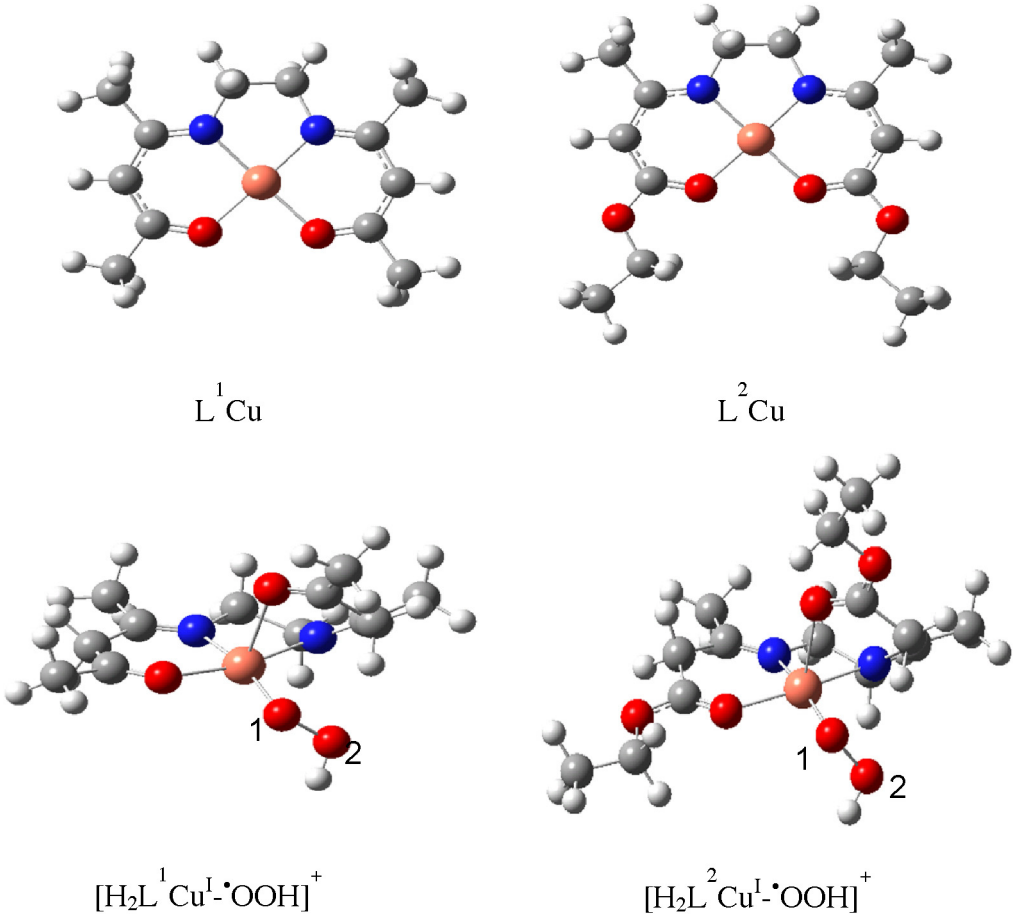

Fig. 7. Optimized geometric configurations of L^1Cu, L^2Cu, $[H_2L^1Cu^{I}\text{-}^{\bullet}OOH]^{+}$ and $[H_2L^2Cu^{I}\text{-}^{\bullet}OOH]^{+}$ (nitrogen atoms are illustrated in blue, oxygen atoms in red and copper atom in orange). (For interpretation of the references to color in this figure legend, the reader is referred to the web version of the article.)

the increase of the reduction current intensity indicated that a new oxidation species formed in the presence of H_2O_2 in a similar manner to other reports early [28,37–40]. It could be observed that the two small reduction waves Ic and IIc, which may be correspond to the state forms of Cu^{2+} and Cu^{+} respectively [41–43], also caused some tiny changes (see Table S1) with the addition of H_2O_2. An obvious phenomenon was that for the two complexes L^1Cu and L^2Cu, both the position and the electric current intensity of the oxidation waves at E_{pla} = 0.311–0.316 V/SCE hardly changed after adding H_2O_2, which was different from those metal complexes reported by literatures [37–39]. It was also found that the new active species possesses relatively high reduction potential (E_{pIIIc}) in aqueous solution at ambient temperature (Table S1). The redox potential of the LCu^{I}-•OOH species is larger than those of most reported metal oxo species [2,23], the species is a more stable than reported radical complexes [44,45] in aqueous solution.

For metal complexes, the properties of ligands generally determine the degree of electron transfer. Owing to the Ligand coordinated with Cu^{2+} was electronic conjugate system, the electron easily transfers within the ligand. Further, it is possible that for the LCu^{I}-•OOH species, the electron could easily transfer among ligand L, Cu^{2+}(or Cu^{+}) and •OOH. Therefore, in the process of LCu^{I}-•OOH species associating and reacting with substrate, the electron and proton H^{+} could easily transfer between the LCu^{I}-•OOH species and substrate.

3.3. Density Functional Theory computation

The geometric configurations of copper (II) complexes LCu, $[H_2LCu^{I}$-•OOH$]^{+}$ (Fig. 7), $[H_2LCu]^{2+}$ and [LCu-OOH]$^{-}$ (Fig. S7) were calculated by using DFT method. The computation results indicate that the geometries of complexes LCu and $[H_2LCu]^{2+}$ are square plane configurations with Cu^{2+} at the center. The geometric configurations of [LCu-OOH]$^{-}$ (Fig. S7) and $[H_2LCu^{I}$-•OOH$]^{+}$ are five-coordinate square pyramidal structures: four atoms including two N atoms, one carbonyl O atom and one hydroperoxo O atom encircle a central Cu^{2+} ion to construct an approximate square plane configuration and one carbonyl O atom is in an axial position. The introduction of hydroperoxo free radical •OOH reorganizes the coordination of Cu^{2+} ion with coordinating other atoms. To our surprise, the hydroperoxo O atom occupies one position of carbonyl O atom and then the carbonyl O atom is arranged at the position of an axial coordination. The calculated distance (1.888–1.898 Å) of Cu atom with hydroperoxo O atom is shorter than that of other four coordination atoms (Table S2), which indicate that the association of hydroperoxo free radical •OOH with copper complex LCu is steady. The axial ligand also plays an important role in the activity for catalysis reaction [46,47]. The DFT calculation displays that the property of copper complex associated hydroperoxo free radical species may be easily changed through the replacement of the axial ligand of carbonyl O atom by other group containing O, N, P or S coordination atom. In this work it was found that when ethanol was added to the LCu/H_2O_2 mixture solution, the UV–vis spectrum recovered its former shape of LCu solution, and the product analysis showed that the ethanol had not be oxidized. This implied that the ethanol may disturb the coordination form of copper complexes, changed the geometric configurations of active species by replacing the axial ligand of carbonyl O atom and resulted in the disappearance of species L^1Cu^{I}-•OOH. This could also explain the sensitivity of species LCu-•OOH as well as reaction to environment. Further we found that the generation of species L^1Cu^{I}-•OOH was sensitive to solution medium, and the tartaric acid played an important role to the generation of this species. Compared with H_2O_2, The O-O bond length in complex $[H_2LCu^{I}$-•OOH$]^{+}$ is slightly shorter (Table S2), which implied that the copper complex could induce the electron transfer of O atoms and activate the free radical •OOH.

4. Conclusions

The reactive species LCu^{I}-•OOH could be generated by reacting copper complexes LCu with H_2O_2 in tartaric acid solution. The reactive species was relatively stable and possesses relatively high oxidation potential in aqueous solution at ambient temperature. The DFT computation results indicated that the geometry of LCu^{I}-•OOH was five-coordinate square-pyramidal configuration and this may lead to the extreme sensitivity of species LCu-•OOH as well as reaction to environment. The copper (II) complexes LCu displayed excellent catalytic ability for the selective oxidation of Mandelic acids (MA, 4-HMA, 4-MMA) into aromatic aldehydes by H_2O_2 in tartaric acid solution.

Supplementary data

Some experimental data and computational data.

Acknowledgments

This work has been supported by the National Natural Science Foundation of China (Nos. 21073126 and 21273156).

Appendix A. Supplementary data

Supplementary data associated with this article can be found, in the online version, at http://dx.doi.org/10.1016/j.molcata.2013.09.004.

References

[1] B.F. Gherman, D.E. Heppner, W.B. Tolman, C.J. Cramer, J. Biol. Inorg. Chem. 11 (2006) 197–205.
[2] S.O. Kim, C.V. Sastri, M.S. Seo, J. Kim, W. Nam, J. Am. Chem. Soc. 127 (2005) 4178–4179.
[3] A. Serafimidou, A. Stamatis, M. Louloudi, Catal. Commun. 9 (2008) 35–39.
[4] R.A. Geiger, D.F. Leto, S. Chattopadhyay, P. Dorlet, E. Anxolabéhère-Mallart, T.A. Jackson, Inorg. Chem. 50 (2011) 10190–10203.
[5] S. Itoh, Curr. Opin. Chem. Biol. 10 (2006) 115–122.
[6] M.R. Maurya, A.K. Chandrakar, S. Chand, J. Mol. Catal. A: Chem. 270 (2007) 225–235.
[7] J.A. Bumpus, M. Tien, D. Wright, S.D. Aust, Science 228 (1985) 1434–1436.
[8] S.T. Prigge, A.S. Kolhekar, B.A. Eipper, R.E. Mains, L.M. Amzel, Science 278 (1997) 1300–1305.
[9] M. Kodera, T. Kita, I. Miura, N. Nakayama, T. Kawata, K. Kano, S. Hirota, J. Am. Chem. Soc. 123 (2001) 7715–7716.
[10] A. Crespo, M.A. Marti, A.E. Roitberg, L.M. Amzel, D.A. Estrin, J. Am. Chem. Soc. 128 (2006) 12817–12828.
[11] K. Yoshizawa, N. Kihara, T. Kamachi, Y. Shiota, Inorg. Chem. 45 (2006) 3034–3041.
[12] A. Decker, E.I. Solomon, Curr. Opin. Chem. Biol. 9 (2005) 152–163.
[13] P. Comba, C. Haaf, S. Helmle, K.D. Karlin, S. Pandian, A. Waleska, Inorg. Chem. 51 (2012) 2841–2851.
[14] Y.J. Choi, K.B. Cho, M. Kubo, T. Ogura, K.D. Karlin, J. Cho, W. Nam, Dalton Trans. 40 (2011) 2234–2241.
[15] T. Fujii, A. Naito, S. Yamaguchi, A. Wada, Y. Funahashi, K. Jitsukawa, S. Nagatomo, T. Kitagawa, H. Masuda, Chem. Commun. (2003) 2700–2701.
[16] S.H. Kim, H. Park, M.S. Seo, M. Kubo, T. Ogura, J. Klajn, D.T. Gryko, J.S. Valentine, W. Nam, J. Am. Chem. Soc. 132 (2010) 14030–14032.
[17] A. Wada, S. Ogo, S. Nagatomo, T. Kitagawa, Y. Watanabe, K. Jitsukawa, H. Masuda, Inorg. Chem. 41 (2002) 616–618.
[18] R. Mas-Balleste, L. Que Jr., J. Am. Chem. Soc. 129 (2007) 15964–15972.
[19] J. Cho, S. Jeon, S.A. Wilson, L.V. Liu, E.A. Kang, J.J. Braymer, M.H. Lim, B. Hedman, K.O. Hodgson, J.S. Valentine, E.I. Solomon, W. Nam, Nature 478 (2011) 502–505.
[20] I. Schepetkin, A. Potapov, A. Khlebnikov, E. Korotkova, A. Lukina, G. Malovichko, L. Kirpotina, M.T. Quinn, J. Biol. Inorg. Chem. 11 (2006) 499–513.
[21] T.Y. Lin, C.H. Wu, J. Catal. 232 (2005) 117–126.
[22] S. Wang, L. Wang, M. Dakovic, Z. Popovic, H. Wu, Y. Liu, ACS Catal. 2 (2012) 230–237.
[23] S. Fukuzumi, L. Tahsini, Y.M. Lee, K. Ohkubo, W. Nam, K.D. Karlin, J. Am. Chem. Soc. 134 (2012) 7025–7035.
[24] E.I. Solomon, P. Chen, M. Metz, S.K. Lee, A.E. Palmer, Angew Chem. Int. Ed. 40 (2001) 4570–4590.
[25] J.M. Li, X.G. Meng, C.W. Hu, J. Du, X.C. Zeng, J. Mol. Catal. A: Chem. 299 (2009) 102–107.
[26] V. Resch, W.M.F. Fabian, W. Kroutil, Adv. Synth. Catal. 352 (2010) 993–997.

[27] M.E. Brown, T. Barros, M.C.Y. Chang, Chem. Biol. 7 (2012) 2074–2081.
[28] E.E. Ferapontova, J. Castillo, L. Gorton, BBA 1760 (2006) 1343–1354.
[29] N. Sathitsuksanoh, A. George, Y.H.P. Zhang, J. Chem. Technol. Biotechnol. 88 (2013) 169–180.
[30] T.Q. Yuan, F. Xu, R.C. Sun, J. Chem. Technol. Biotechnol. 88 (2013) 346–352.
[31] W.P. Zeng, X.H. Li, J. Du, J.M. Li, P. Zhang, C.W. Hu, X.G. Meng, Acta Chim. Sinica 68 (2010) 27–32.
[32] B. Liu, X.G. Meng, W.Y. Li, L.C. Zhou, C.W. Hu, J. Phys. Chem. A 116 (2012) 2920–2926.
[33] A.E. Martell, R.L. Belford, M. Calvin, J. Inorg. Nucl. Chem. 5 (1958) 170–181.
[34] C.K.Z. Andrade, A.F.S. Barreto, W.A. Silva, Arkivoc 7 (2008) 226–232.
[35] L. Mouni, M. Akkurt, S.O. Yıldırım, T.B. Hadda, Z.H. Chohan, J. Chem. Crystallogr. 40 (2010) 169–172.
[36] J.P. Costes, J.P. Laurent, Inorg. Chem. 27 (1988) 3235–3237.
[37] C.V. Sastri, K. Oh, Y.J. Lee, M.S. Seo, W. Shin, W. Nam, Angew. Chem. Int. Ed. 45 (2006) 3992–3995.
[38] M. Senel, E. Cevik, M.F. Abasıyanık, Sens. Actuator B: Chem. 145 (2010) 444–450.
[39] Q. Yu, Z.S. Shi, X.Y. Liu, S.L. Luo, W.Z. Wei, J. Electroanal. Chem. 655 (2011) 92–95.
[40] V.L.N. Dias, E.N. da Fernandes, L.M.S. Silva, E.P. Marques, J.J. Zhang, A.L. Brandes Marques, J. Power Sources 142 (2005) 10–17.
[41] M. Meyer, L. Fremond, E. Espinosa, R. Guilard, Z. Ou, K.M. Kadish, Inorg. Chem. 43 (2004) 5572–5587.
[42] A.M. Lazarin, C.A. Borgo, Y. Gushikem, J. Membr. Sci. 221 (2003) 175–184.
[43] K.K. Sarker, S.S. Halder, D. Banerjee, T.K. Mondal, A.R. Paital, P.K. Nanda, P. Raghavaiah, C. Sinha, Inorg. Chim. Acta 363 (2010) 2955–2964.
[44] K. Nakahara, S. Iwasa, J. Iriyama, Y. Morioka, M. Suguro, M. Satoh, E.J. Cairns, Electrochim. Acta 52 (2006) 921–927.
[45] F.S. de Paula, A.G. Cioletti, J.F. da Silva Filho, A.E.G. Santana, A.F. dos Santos, M.O.F. Goulart, M. Vallaro, R. Fruttero, J. Electroanal. Chem. 544 (2003) 25–34.
[46] L. Duan, F. Bozoglian, S. Mandal, B. Stewart, T. Privalov, A. Llobet, L. Sun, Nat. Chem. 4 (2012) 418–423.
[47] J.L. Fillol, Z. Codola, I. Garcia-Bosch, L. Gomez, J.J. Pla, M. Costas, Nat. Chem. 3 (2011) 807–813.